View metadata, citation and similar papers at core.ac.uk

brought to you by CORE

provided by Cronfa at Swansea University

Cronfa - Swansea University Open Access Repository

This is an author produced version of a paper published in :
Microelectronics Reliability

Cronfa URL for this paper:
http://cronfa.swan.ac.uk/Record/cronfa22172

Paper:

Eckermann, J., Mehmood, S., Davies, H., Lavery, N., Brown, S., Sienz, J., Jones, A. & Sommerfeld, P. (2014). Computational modeling of creep-based fatigue as a means of selecting lead-free solder alloys. *Microelectronics Reliability, 54*(6-7), 1235-1242.

http://dx.doi.org/10.1016/j.microrel.2014.02.017

This article is brought to you by Swansea University. Any person downloading material is agreeing to abide by the terms of the repository licence. Authors are personally responsible for adhering to publisher restrictions or conditions. When uploading content they are required to comply with their publisher agreement and the SHERPA RoMEO database to judge whether or not it is copyright safe to add this version of the paper to this repository.
http://www.swansea.ac.uk/iss/researchsupport/cronfa-support/

Microelectronics Reliability 54 (2014) 1235–1242

Contents lists available at ScienceDirect

Microelectronics Reliability

journal homepage: www.elsevier.com/locate/microrel

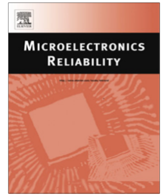

Computational modeling of creep-based fatigue as a means of selecting lead-free solder alloys

J. Eckermann [a,*], S. Mehmood [a], H.M. Davies [a], N.P. Lavery [a], S.G.R. Brown [a], J. Sienz [a], A. Jones [b], P. Sommerfeld [b]

[a] Advanced Sustainable Manufacturing Technologies (ASTUTE), College of Engineering, Swansea University, Singleton Park, Swansea SA2 8PP, United Kingdom
[b] Electronic Motion Systems UK Ltd., Heol-y-Ddraig, Penllergaer Business Park, Penllergaer, Swansea SA4 9HL, United Kingdom

ARTICLE INFO

Article history:
Received 18 September 2013
Received in revised form 5 February 2014
Accepted 23 February 2014
Available online 29 March 2014

Keywords:
Lead-free solders
SAC305
Creep
Fatigue
Anand-Model
Coffin–Manson

ABSTRACT

The primary aim of this investigation was to understand the effect of temperature fluctuations on a number of various solder materials namely SAC105, SAC305, SAC405 and Sn–36Pb–2Ag. To achieve this objective, three different classic joint assemblies (a ball joint, a test specimen joint and finger lead joint) were modeled which provided the foundation for the creep and fatigue behaviors simulation. Anand's viscoplasticity as a constitutive equation was employed to characterize the behavior of solders numerically under the influence of thermal power cycles (80–150 °C) and thermal shock cycles (−40 to 125 °C). To extend the research outcome for industrial use, two additional research activities were carried out. One of them was to obtain lifetime-predictions of solder joints based on Coffin Manson concept. The other one focused on parameterization to obtain the ideal solder thickness under the consideration of plastic strain and economic benefit.

© 2014 Elsevier Ltd. All rights reserved.

1. Introduction

Solders, made of fusible metal alloys, are used to join two parts together in an electronic assembly. Apart from the mechanical bonding, they also provide an electrical interconnection between the two parts [1]. Due to the differences in material properties such as the coefficients of thermal expansion (CTE) of the metal parts, thermal stresses arise in the assembly, which consequently lead to a reduction in the lifetime of the joint [2]. In thermal fatigue, there is a transition from fatigue failure to creep failure as the temperature increases (creep dominates at higher temperature) and the situation becomes even more complicated if both fatigue and creep interact with each other during thermal or power cycling of electronic packages.

Lead based solders have been used for many years in the industry because of their good material properties. Due to the new legislation "Restriction of Hazardous Substances Directive" in 2006, lead based solders are gradually being replaced by lead free solders in the electronic industry [3]. At present, the creep behavior and lifetime expectation of these lead free solders are not well understood under the influence of temperature fluctuations. Therefore, much effort is being expended in time-consuming experimental investigations to obtain data on the creep behavior and the lifetime expectation.

The literature review highlighted three typical but different joint assemblies (a ball joint, a test specimen joint and finger lead joint) for which clear joint geometry, solder properties and loading cycles were given, in conjunction with experimental test data. With this combination of test case information, it was possible to run a series of simulations using Anand's viscoplasticity model to gain information about the impact of temperature fluctuations on different solders. Empirical methods were then used to predict the life of these joints in terms of the number of cycles to failure ($\mathbf{N_f}$).

In our view this paper will provide a starting point from which other researchers can obtain geometry, material properties and boundary conditions to benchmark their own use of computational creep models of lead-free solders. In comparison to the previous work, this investigation provides a good assessment of various solder behaviors in different geometries and load cycles under a constant simulation settings.

2. Modeling methodology and benchmark simulations

A printed circuit board (PCB) is an electronic assembly in which electronic chips or leads are fastened via solder joints [4]. Such assemblies play an important role for computers [5] and other

* Corresponding author. Tel.: +44 1792 606881.
E-mail address: J.Eckermann@swansea.ac.uk (J. Eckermann).

http://dx.doi.org/10.1016/j.microrel.2014.02.017
0026-2714/© 2014 Elsevier Ltd. All rights reserved.

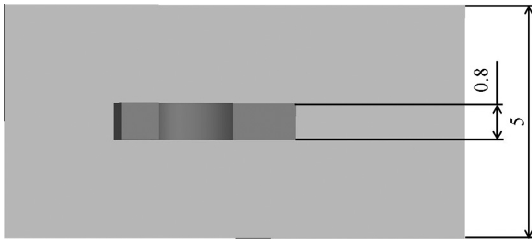

Fig. 1. Finger lead model (top view).

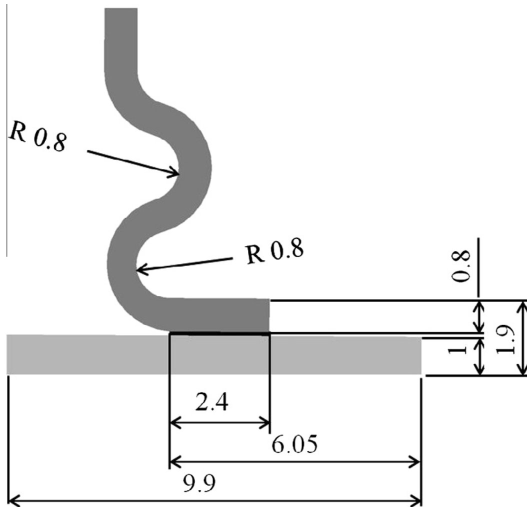

Fig. 2. Finger lead joint (front view).

appliances. Therefore, three of the most widely used solder joint models were chosen and designed after reviewing current literature. Figs. 1 and 2 illustrate the finger lead joint made of a copper finger lead, a thin solder layer (thickness of 200 μm, length of 2400 μm and width of 800 μm) and a copper plate. The test specimen joint (Fig. 3) whose geometry was also used by [6], consisted of two identical sized copper plates and a thin solder layer (thickness of 180 μm, width of 1000 μm and length of 3000 μm). The ball solder joint (Fig. 4) as described in [7,8] is used in the Ball Grid Array (BGA) assembly, and consists of two identical sized copper plates and a solder ball (width of 0.484 mm, top diameter of 0.484 mm and Ball diameter of 0.744 mm).

Modeling is an extremely useful tool in the early design stage to reduce the cost and time of testing. The accuracy of the results

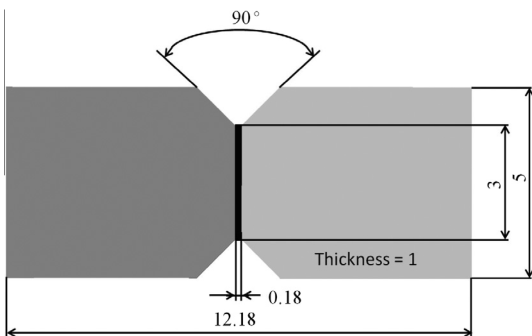

Fig. 3. Test specimen joint.

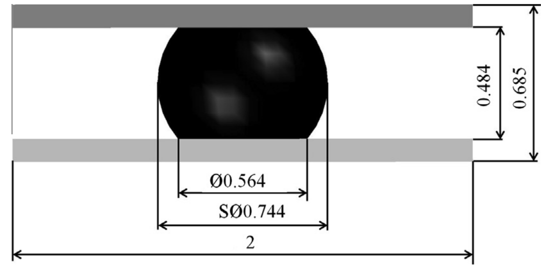

Fig. 4. Ball joint.

significantly depends on the choice of the constitutive equations employed and the material parameters used for modeling [9].

2.1. Visco-plastic models

In general, the unified viscoplastic model considers the inelastic strain rate variation by using a flow law and the variation of the state variables described by evolution equations. Some unified viscoplastic models are the Anand model, McDowell model, Basaran et al., Wei et al. and Chaboche's model. The Anand model is one of the simplest models which can be implemented in the FE codes. Chaboche's viscoplastic model includes combined kinematic/isotropic hardening effects whereas Anand model considers only the isotropic hardening effects. McDowell's model comprises the features of Anand model and Chaboche's model. It uses the Zener Hollowman parameter for creep activation mechanisms and combined kinematic/isotropic hardening [10].

2.2. Anand model

Anand is a common alternative model to creep for simulation of viscoplastic behavior in solders. Many previous simulations have been carried out with the Anand model and published [11,12]. The Anand model is expressed by a flow equation and three evolution equations, as written mathematically below.

Flow equation

$$\dot{\varepsilon}_{\mathbf{p}} = \mathbf{A}\ \exp\left(-\frac{Q}{RT}\right)\left[\sinh\left(\xi\frac{\sigma}{s}\right)\right]^{1/\mathbf{m}} \tag{1}$$

where $\dot{\varepsilon}_{\mathbf{p}}$ represents the inelastic strain rate, $\mathbf{A}$ is a pre-exponential factor, Q is used for the activation energy, R stands for gas constant, T is absolute temperature, ξ is the multiplier of stress, σ is the equivalent stress, $\mathbf{m}$ is strain rate sensitivity.

Evolution equations

$$\dot{\mathbf{s}} = \left\{\mathbf{h}_0(|\mathbf{B}|)^{\mathbf{a}}\frac{\mathbf{B}}{|\mathbf{B}|}\right\}\dot{\varepsilon}_{\mathbf{p}} \tag{2}$$

where

Table 1
Anand parameters for various solders [12,13].

Symbol	Units	SAC105	SCA305	SAC405	Sn36Pb2Ag
$\mathbf{S}_0$	MPa	2.348	2.150	1.3	12.41
Q/R	K^{-1}	8076	9970	9000	9400
A	S^{-1}	3.773	17.994	500	4000000
ξ		0.995	0.350	7.100	1.5
M		0.445	0.153	0.300	0.303
$\mathbf{h}_0$	MPa	4507.5	1525.98	5900	1379
$\hat{\mathbf{S}}$	MPa	3.583	2.536	39.4	13.79
N		0.012	0.028	0.030	0.07
A		2.167	1.690	1.100	1.3

Table 2
Material properties of solders and copper.

Material Properties	Units	Solder			
		SAC105 [13,14]	SAC305 [13,15]	SAC405 [16,15]	Sn36Pb2Ag [17]
Density	kg m^{-3}	7334.2	7400	7440	8410
CTE	K^{-1}	1.95E−05	2.00E−05	2.00E−05	2.40E−05
Young's modulus	Pa	4.41E+10	5.12E+10	4.46E+10	3.36E+10
Poison's ratio	–	0.42	0.4	0.42	0.4
Tensile yield strength	Pa	2.27E+07	3.35E+07	2.85E+07	3.02E+07
Compressive yield strength	Pa	2.88E+07	2.96E+07	3.19E+07	3.12E+07
Tensile ultimate strength	Pa	2.93E+07	3.95E+07	3.99E+07	3.39E+07
Compressive ultimate strength	Pa	4.94E+07	5.85E+07	3.62E+07	4.94E+07

Material Properties	Units	Copper [17]
Density	kg m^{-3}	8960
CTE	K^{-1}	1.70E−05
Young's modulus	Pa	1.28E+11
Poison's ratio	–	0.34
Tensile yield strength	Pa	7.00E+07
Compressive yield strength	Pa	6.90E+07
Tensile ultimate strength	Pa	2.20E+08

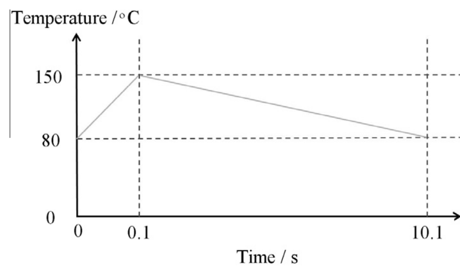

Fig. 5. Power cycle (80–150 °C).

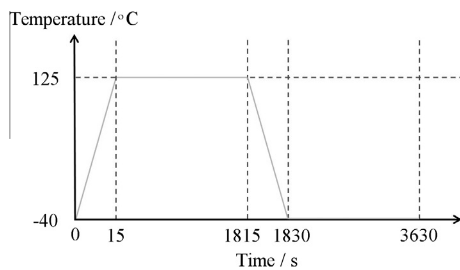

Fig. 6. Thermal shock cycle (−40 to 125 °C).

$$\mathbf{B} = 1 - \frac{s}{s^*} \quad (3)$$

And s^* can be determined mathematically using

$$s^* = \hat{s}\left[\frac{\dot{\varepsilon}_\mathbf{p}}{\mathbf{A}} \exp\left(\frac{Q}{RT}\right)\right]^\mathbf{n} \quad (4)$$

In this case, the hardening/softening is abbreviated by $\mathbf{h}_0$, whose strain rate sensitivity is shorten by a. s^* represents a saturation value of deformation resistance s, and $\mathbf{n}$ is the strain rate sensitivity for the saturation value of deformation resistance. Some of the Anand parameters used for the simulations are shown in Table 1.

The material properties used for the simulation are listed in Table 2.

The finite element program ANSYS workbench 14.0 was employed to simulate the creep and fatigue behavior for various types of solders including hypoeutectic lead-free solders SAC105, SAC305, SAC405 and lead solder Sn–36Pb–2Ag. Two types of temperature loadings were used in the models, namely thermal power cycles (80–150 °C) and thermal shock cycles (−40 to 125 °C). This loading impact on the materials was simulated by using the constitutive equation based on Anand's viscoplasticity model. The temperature profile for thermal power cycles (80–150 °C) followed a typical zigzag profile (Fig. 5) whose first ramp up rate of 700 °C/s heats up the assembly from 80 °C to 150 °C within 0.1 s followed by a second cooling rate of 7 °C/s for 10 s. For the thermal shock profile (Fig. 6), the ramp rates for heating and cooling the assembly between the temperature extremes of −40 °C and 125 °C takes 15 s. The dwell time for both extremes is 30 min.

The 3D models were meshed structurally using solid 186 elements (Fig. 7) which were defined by 20 nodes and allowed to exhibit quadratic displacement behavior [18]. The minimum number of substeps was set at 5 and the maximum number was 20 for all load steps using the multistep function available in workbench 14.0.

2.3. Life prediction models

The concept of the fatigue life models is to determine the number of cycles that an assembly can endure before failure. Several fatigue models were investigated and proposed to predict the fatigue life on the basis of [19]:

- Stress.
- Strain energy density.
- Creep strain.
- Damage mechanics.

The Palmgren–Miner rule predicts the fatigue life based on the assumption of linear accumulation of damage in specimens subjected to variable amplitude (VA) loading [16]. The

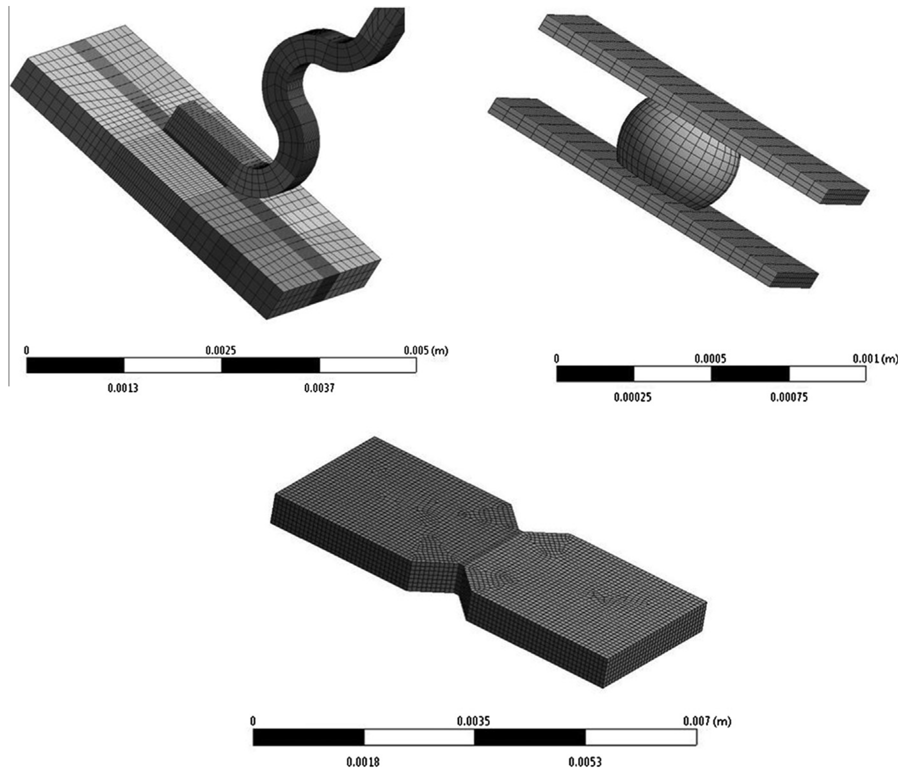

Fig. 7. Mesh element used in modeling.

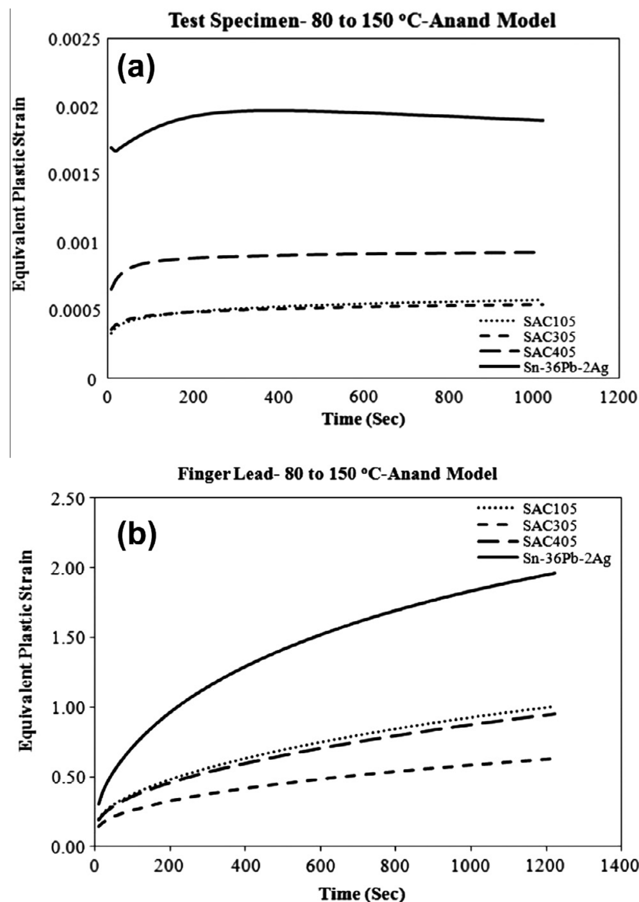

Fig. 8. Equivalent plastic strain for various solders in test specimen (a) and finger lead design (b) under power cycling using Anand model.

Monkmann–Grant method is used to calculate the time of rupture based on creep. This method belongs to the category of the primary damage mechanism [23].

Strain based models take into consideration of the loss of ductility in the solders and probably be more suitable for ductile solders such as leaded solders. Strain energy density based criterion emphasize on the strength and ductility of the solder and be more applicable to modern Sn–Cu–Ag solders. Damage mechanics deals with the concept of crack initiation and propagation in solders. In general, different models are suitable for different scenarios, but common practice is to use them concurrently. For this analysis, the Coffin–Manson model was used to calculate the number of cycles to failure ($\mathbf{N_f}$) because of its simplicity and reliability in other applications [9,20,21,22]. According to this method, the total number of cycles to failure can be defined by either Creep Strain or Creep Energy Density through the following relations [20]:

$$\mathbf{N_f} = \mathbf{A}(\Delta\varepsilon_{\mathbf{cr}})^{\mathbf{B}} \tag{5}$$

$$\mathbf{N_f} = \mathbf{C}(\Delta\mathbf{W_{cr}})^{\mathbf{D}} \tag{6}$$

where **A** and **B** are the material constants. The term $\Delta\varepsilon_{\mathbf{cr}}$ is known as creep strain, but in our case it is equivalent plastic strain, which can be obtained from FEM simulations for each individual load step. Equivalent plastic strain obtained from FEM simulations contains two strain components: time dependent creep strain and time independent plastic strain. For the sake of our analysis it was not possible to isolate true creep strain components. In this case, the hardening effect will be considered in the Anand model used in the previous stage. Once the above values are known, the life prediction curves can be plotted. An accurate life prediction can be achieved when a simulation runs with constants whose

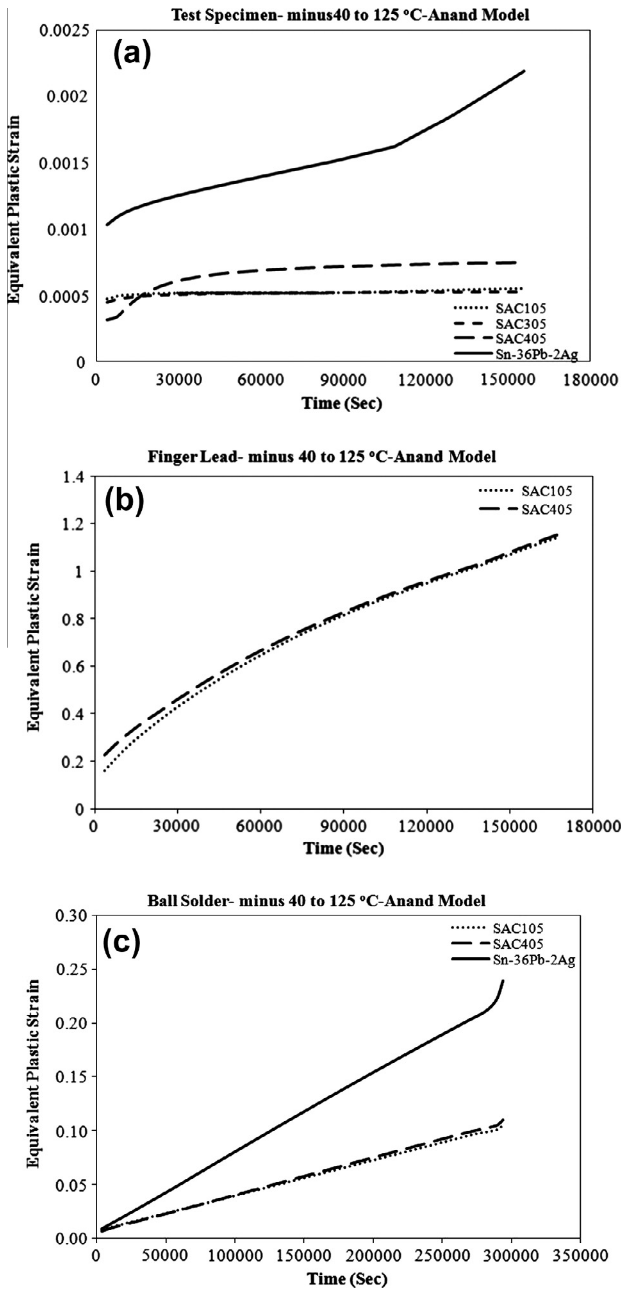

Fig. 9. Equivalent plastic strain for various solders in test specimen (a) and finger lead design (b) and ball solder design (c) under thermal shock cycling using Anand model.

values were experimentally derived from similar boundary conditions to those used in the simulation [19].

3. Results and discussions

Simulations for the finger lead benchmark with ternary tin–silver–copper solders SAC105, SAC305, SAC405 and a lead solder Sn36Pb–2Ag, were carried out using the Anand constitutive equation. Fig. 8 shows several plastic strain creep curves of different solders used for test specimen and finger lead model. The strain-time curve shows two distinctive regions. In the first region, an initial high strain rate slows down with increased time until it almost becomes constant where a balance between work hardening and the recovery process occurs.

As seen from the comparative results in Fig. 8a and b, SAC305 has the highest creep resistance among the solders followed by either SAC105 or SAC405 and Sn36Pb–2Ag. SAC405 has a lower creep resistance than SAC305 which does not conform to the experimental results. It has been shown in the literature that the increased silver content prevents shear plastic deformation of the solder bump [24]. However, some of the outcomes reflect the conclusions drawn from experimental results. For example, it was noticed from the experimental outcome that SAC105 has a very good creep resistance compared to the lead solders at lower stress, which was also shown from the simulations [25].

Another conclusion drawn by Ref. [7] was that SAC105 exhibits a poor thermal cycling performance in comparison to SAC305, which is also reflected in the current results.

Fig. 9 illustrates several plastic strain curves obtained by simulations with finger lead, test specimen and ball joints using Anand model under the thermal shock condition. The outcomes are similar to the results from the power cycles conditions in terms of the relative creep resistance of the solders used.

The contour plots of the Equivalent von-Mises stresses are shown in Fig. 10 for the three benchmark problems, exposed to different thermal cycles: test specimen (a), finger lead (b) and ball solder (c). The evolution of maximum stresses in the finger lead occurred at the corners whereas in the test specimen and ball solder the maximum stress developed at the interface between the solder and copper plates.

The finger lead benchmark with SAC105 solder was simulated under different thermal loadings to answer the question "Which of the thermal cycles generated more strain in the joint?" The answer of this question was that the power cycle developed a faster plastic strain accumulation than the thermal shock cycle illustrated in Fig. 11.

To predict the lifetimes of SAC305 and Sn–36Pb–2Ag, the results from the finger lead simulation under the power cycle were used with the parameters listed in Table 3.

As can be seen in Fig. 12, SAC305 had a shorter lifetime than the lead solder under the power cycle condition at the lower strain range whereas at the higher strain range, lead solder has a shorter lifetime in comparison with lead free solder SAC305.

A parameterization study was conducted with the objective to obtain a minimum plastic strain as a function of solder thickness. Hereby, the Anand parameters for SAC105, SAC305, SAC405 and Sn–36Pb–2Ag and the material thickness between 0.1 mm and 0.5 mm were used for this investigation.

As can be seen in Fig. 8a and b, the strain rate values of different geometries and load cycles vary with a factor of 1000.

To determine then the $\mathbf{N_f}$ for all models despite the huge variation, two different strain ranges were selected namely 0.0004 and 0.05. The values of $\mathbf{N_f}$ at strain range 0.0004 are listed in Tables 4 and Table 5 listed the values of $\mathbf{N_f}$ at strain range 0.05.

As seen in Fig. 13, the equivalent plastic strain in all solders falls steeply between 0.1 mm and 0.3 mm. After thickness of 0.3 mm, the equivalent plastic strain decreases at a slow rate. The significant finding to emerge from this research activity is that the solder thickness also plays an important part in the outcome of the joint reliability. In respect of cost versus lifetime, a thickness of 0.3 mm might be the ideal solution.

4. Conclusions

- The results of Sn36Pb2Ag, SAC105 and SAC305 were in good agreement with the conclusions from other experimental work in terms of the increasing order of creep resistance. Interestingly, SAC405 did not follow the trend.

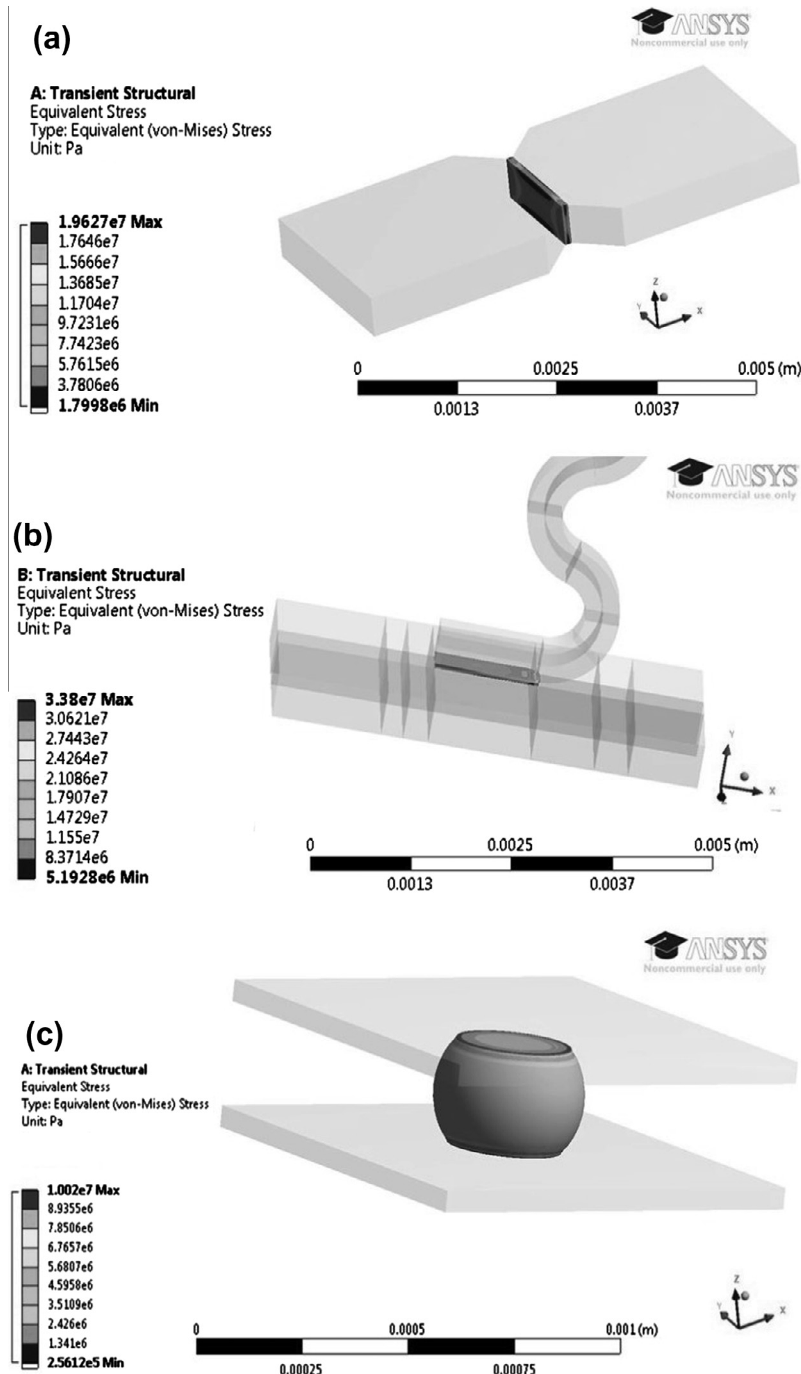

Fig. 10. Equivalent von-Mises stress for various solders in test specimen with thermal shock (a) and finger lead design with power cycle (b) and ball solder design with thermal shock (c) using Anand model.

- The creep behavior of the lead free solders was successfully simulated for all models under the power cycles and thermal shock cycles loadings. Surprisingly, it was not possible to simulate the creep behavior of lead solder used in the finger lead model under thermal shock.
- Corners and interfaces are the areas where solders experience the maximum stresses.
- Power cycles develop higher strain in the joints in comparison with thermal shock cycles.
- Whilst there is a large amount of prior work, detailed benchmark case studies with clear geometry, material properties and experimental data have been hard to come by, and would justify future work concentrating on such benchmarks specifically for model validation purposes.

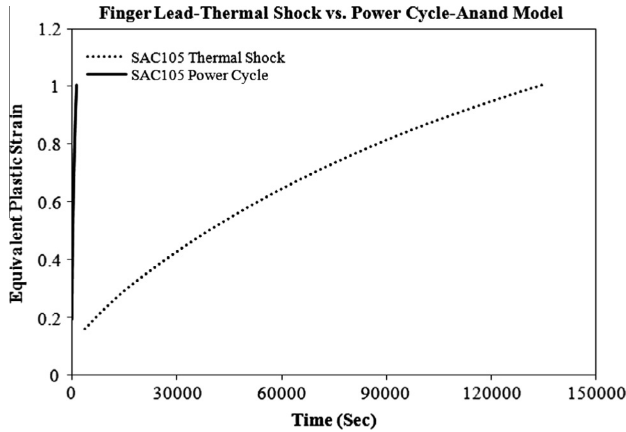

Fig. 11. Equivalent plastic strain for (SAC105) in finger lead design under power vs. thermal cycling using Anand model.

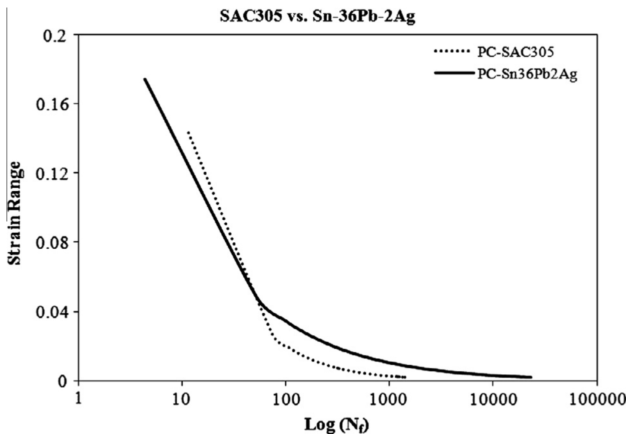

Fig. 12. Coffin Manson life curves (finger lead benchmark) for SAC305 vs. Sn–36Pb–2Ag under power cycling using Anand model.

Table 3
Coffin–Manson parameters for life prediction [21].

Solder	A	B
SAC305	0.7188	1.1093
Sn–36Pb–2Ag	0.146	1.94

Table 4
Number of cycles to failure at strain range of 0.0004.

	Power		Thermal	
	SAC305	Sn–36Pb–2Ag	SAC305	Sn–36Pb–2Ag
Finger lead	–	–	Infinity	–
Ball solder	5200	0.5E+6	–	–
Test specimen	N/A	1.0E+6	1.0E+6	1.2E+6

Table 5
Number of cycles to failure at strain range of 0.05.

	Power		Thermal	
	SAC305	Sn–36Pb–2Ag	SAC305	Sn–36Pb–2Ag
Finger lead	60	Infinity	660	N/A
Ball solder	–	–	Infinity	400
Test specimen	–	–	–	–

– No data available.

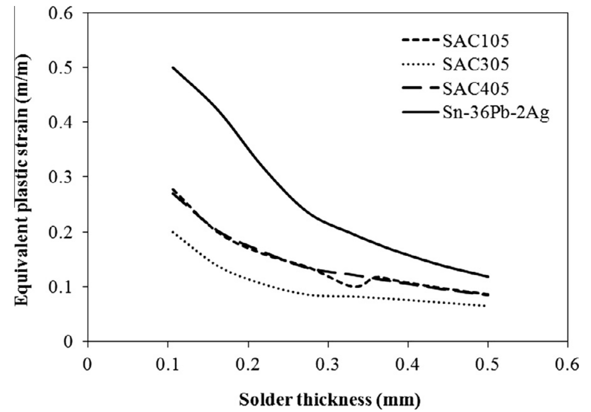

Fig. 13. Effect of solder thickness on equivalent plastic strain for different solders in finger lead design under power cycling.

- The parameterization study emphasized the important factor of solder thickness for joint reliability.
- This research has highlighted many questions about the material properties, which need further investigation. It would be ideal to obtain material properties with the same temperature profile used for the simulation.

Acknowledgments

The work described in this paper was carried out as part of the *Advanced Sustainable Manufacturing Technologies* (ASTUTE) project (Ref. No. 80380) in collaboration with Electronic Motion Systems, whom the authors would like to thank for their inputs. ASTUTE has been part-funded by the European Regional Development Fund through the Welsh Government, and the authors would like to acknowledge this funding.

References

[1] Pang JH, Che F. Thermal fatigue reliability analysis for PBGA with Sn–3.8Ag–0.7Cu solder joints. Electron Packaging Technol Conf 2004.
[2] Siewert T, Liu S, Smith DR, Madeni JC. Database for solder properties with emphasis on new lead-free solders. NIST & Colorado School of Mines, Release 4.0, Feb. 2002. <http://www.boulder.nist.gov/div853/lead free/solders.html>.
[3] Available: http://ec.europa.eu/environment/waste/rohs_eee/.
[4] Liang Z, Ji-guang H, Cheng-wen H, Yong-huan G. Reliability behaviour of lead-free solder joints in electronic components. J Mater Sci: Mater Electron 2013;24(1).
[5] Yang L, Bernstein JB, Koschmieder T. Assessment of acceleration models used for BGA solder joint reliability studies. Microelectron Reliab 2009;49(12):1546–54.
[6] Burke C, Punch J. A comparison of the creep behavior of joint-scale SAC105 and SAC305 solder samples under shear conditions. In: Thermal, mechanical and multi-physics simulation and experiments in microelectronics and microsystems (EuroSimE), 13th International Conference; 2012.
[7] Bhate D, Chan D, Subbarayan G, Chiu TC, Gupta V, Edwards DR. Constitutive behavior of Sn3.8Ag0.7Cu and Sn1.0Ag0.5Cu alloys at creep and low strain rate regimes. IEEE Trans Compon Packaging Technol 2008;31(3):622–33.
[8] Che FX, Pang JH. Characterization of IMC layer and its effect on thermomechanical fatigue life of Sn–3.8Ag–0.7Cu solder joints. J Alloys Compd 2012;541:6–13.
[9] Ridout S, Bailey C. Review of methods to predict solder joint reliability under thermo-mechanical cycling. Fatigue Fract Eng Mater Struct 2007;30(5):400–12.
[10] Msolli S, Zeanh A, Dalverny O, Karama M. Efficiency and robustness of some behavior laws in the description of. In: International conference on thermal mechanical and multiphysics simulation and experiments in mirco-electronics and micro-systems, EuroSimE2010, Bordeaux; 2010.
[11] Wang GZ, Cheng ZN, Becker K, Wilde J. Applying Anand model to represent the viscoplastic deformation behavior of solder alloys. J Electro Packaging 2001;123(3):247–53.
[12] Wang Q, Zhang Y, Liang L, Liu Y, Irving S. Anand parameter test for Pb-free material SnAgCu and life prediction for a CSP. Electron Packaging Technol 2007:1–9.

[13] El-Daly AA, El-Tantawy F, Hammad AE, Gaafar MS, El-Mossalamy EH, Al-Ghamdie AA. Structural and elastic properties of eutectic Sn–Cu lead-free solder alloy containing small amount of Ag and In. J Alloys Compd 2011;509:7238–46.
[14] Che FX, Zhu WH, Poth ES, Zhang XW, Zhang XR. The study of mechanical properties of Sn–Ag–Cu lead-free solders with different Ag contents and Ni doping under different strain rates and temperatures. J Alloys Compd 2010;507(1):215–24.
[15] Nguyen TT, Yu D, Park SB. Characterizing the mechanical properties of actual SAC105, SAC305, and SAC405 solder joints by digital image correlation. J Electron Mater 2011;40(6):1409–15.
[16] Hongtao M. Characterization of lead-free solders for electronic packaging. Auburn: Auburn University Theses and Dissertations; 2007.
[17] Database for solder properties with emphasis on new lead-free solders, National Institute of Standards and Technology; 2013.
[18] A. Syed. Updated life prediction models for solder joints with removal of modelling assumptions and effects of constitutive equations. In: 7th International conference on thermal, mechanical and multiphysics simulation and experiments in micro-electronics and micro-systems, EuroSime; 2006.
[19] Lee WW, Nguyen LT, Selvaduray GS. Solder joint fatigue models: review and applicability to chip scale packages. Microelectron Reliab 2000;40(2):231–44.
[20] Hannach T, Worrack H, Muller WH, Hauck T. Creep in microelectronic solder joints: finite element simulations versus semi-analytical methods. Arch Appl Mech 2009;79(6–7).
[21] Chiou Y-C, Jen Y-M, Huang S-H. Finite element based fatigue life estimation of solder joints with effect on intermetallic compound growth. Microelectron Reliab 2011;51:2319–29.
[22] Lin J-C, Chiang K-N. Thermal/mechanical analysis of novel ceramic-TSOP using nonlinear finite element method. J Chin Inst Eng 2001;24(4):453–62.
[23] Syed A. Accumulated creep strain and energy density based thermal fatigue life prediction models for SnAgCu solder joints. In: Electronic components and technology conference proceedings 54th; 2004.
[24] Kariya Y, Hosoi T, Terashima S, Tanaka M, Otsuka M. Effect of silver content on the shear fatigue properties of Sn–Ag–Cu flip–chip interconnects. J Elelctron Mater 2004;33(4):321–8.
[25] Mysore K, Subbarayan G. Constitutive and aging behavior of Sn3.0Ag0.5Cu solder alloy. IEEE Trans Electron Packaging Manuf 2009;32(4):221–32.